Phenomenological modelling of solid/liquid phase transitions in non-ideal PCM

Tilman Barz[1], Johann Emhofer[1], Klemens Marx[1], Gabriel Zsembinszki[2], Luisa F. Cabeza[2]

[1]AIT Austrian Institute of Technology GmbH, Center for Energy, Giefinggasse 2, 1210 Vienna, Austria, e-mail: tilman.barz@ait.ac.at.
[2]GREiA Research Group, INSPIRES Research Centre, University of Lleida, Pere de Cabrera s/n, 25001, Lleida, Spain.

Abstract

Thermal energy storage technologies through solid/liquid phase change materials (PCMs) use the thermodynamic principles of melting and solidification to absorb and release thermal energy. In the ideal case, this technology allows to charge and discharge relatively high amounts of thermal energy at a constant, unique temperature. However, for most commercially available technical-grade solid/liquid PCMs melting and solidification cannot be assigned to a single, unique temperature. Instead, the phase transition takes place over a temperature range in which solid and liquid phases coexist. Moreover, supercooling sometimes causes hysteresis in the phase transitions depending on the applied heating and cooling rates. These phenomena cause non-ideal phase transition behaviour and generally reduce the applicability of the PCMs. PCM models which can reproduce this non-ideal behaviour are crucial for the numerical analysis of the charging and discharging operation of latent heat storages. This contribution presents a generic workflow for the identification of phase transition models for industrial-grade solid/liquid PCMs. Adopting a purely phenomenological approach models are directly identified from PCM heat capacity measurement data. Thus, if the data contains information on temperature ranges with coexisting phases and hysteresis in the temperature induced phase transitions these phenomena are directly accounted for. The identified transition models predict liquid mass phase fractions using PCM temperature as a model input. These models are then used to describe apparent (effective) PCM properties in the phase transition temperature range, i.e. specific heat, density and thermal conductivity. Applications of the workflow are presented for different commercial PCMs from Climator Sweden AB. The effects of non-ideal phase transition behaviour on absorption and release of heat in a latent thermal energy storage are discussed by simulation studies.

Keywords: Phase change materials; phase transition models; temperature induced hysteresis; apparent and effective material properties

1. Introduction

The performance of a latent heat thermal energy storage with solid/liquid phase change material (PCM) critically depends on the thermo-physical PCM properties and its phase transition behaviour. However, established simulation tools, for example those for building performance simulation, mostly ignore complex phase transition characteristics, relevant for many technical-grade PCM used in real applications (Al-Saadi and Zhai 2013). One of the major shortcomings of these simulation tools is the lack of suitable models for the description of thermal hysteresis (Goia et al. 2018). Thermal hysteresis effects are complex in nature. They are normally induced

by supercooling which is caused by complex nucleation and crystal growth mechanisms. Uzan et al. 2017 give an interesting introduction to mechanistic modelling approaches and an example to the mechanistic macroscopic modelling of solidification with supercooling.

In contrast to the mechanistic modelling approach for the analysis of hysteresis in the solid/liquid phase transition of PCM, this contribution focusses on a purely phenomenological (data-based) approach without consideration of physical processes inside the PCM. An example can be found e.g. in Goia et al. 2018, where different phenomenological phase transition models are implemented in two different building simulation software (EnergyPlus[TM] and Wufi®Pro/Plus). These models are defined by enthalpy-temperature curves. The curves are derived from the PCM heat capacity data obtained from a differential scanning calorimetry (DSC) for complete melting and solidification. Similar phenomenological models were implemented in COMSOL Multiphysics®, see e.g. Biswas et al. 2018, and Hu and Heiselberg 2018. An alternative phenomenological modelling approach for the consideration of hysteresis was proposed by Gowreesunker and Tassou 2013 and implemented in ANSYS Fluent (Kumarasamy et al. 2017). The so called 'source term' approach uses a heat source term in the PCM energy balance equation model to represent the latent heat during phase change. Similar as for the enthalpy-temperature curves, the model of the source term is derived from DSC heat capacity data obtained for complete melting and for complete solidification. All mentioned approaches are restricted to the analysis of hysteresis effects for complete melting and solidification experiments. The models realize (or track) enthalpy-temperature transition curves identified either for complete melting, complete solidification, or an average between both curves. The main drawback of the so called 'curve track' models is its poor performance when applied to predict phase transition behaviour with hysteresis for partial melting and solidification, see e.g. Diaconu and Cruceru 2010; Moreles et al. 2018; Gasia et al. 2018; Goia et al. 2018.

Because of this reason, based on experimental findings, an extension of the 'curve track' model was proposed by Bony and Citherlet 2007 which realizes a switch from one transition curve to the other for direction changes in the temperature during incomplete phase transitions (so called 'curve switch' model). This approach was taken up by Rose et al. 2009, and was also implemented in NRGsim, a custom sub-routine developed for EnergyPlus[TM]. Moreover, Diaconu et al. 2010 found experimentally that the hysteresis magnitude decreased in the case of temperature cycling inside the PCM phase transition temperature range. They also found that the temperature history influences the enthalpy values. A phenomenological model which accounts for different hysteresis magnitudes for cycles within the PCM phase transition temperature range, and which makes use of the temperature history was presented recently by Barz and Sommer 2018. It can be applied for the prediction of phase transitions during consecutive partial melting and solidification and is referred to here as 'curve scale' model.

This contribution adopts the 'curve scale' modelling approach and presents a workflow for the identification of corresponding phase transition models for industrial-grade solid/liquid PCMs. The model is directly identified from PCM heat capacity measurement data. If the data contains information on temperature ranges with coexisting phases and hysteresis in the temperature induced phase transitions these phenomena are directly accounted for. The steps for model identification are presented and exemplarily applied to commercial PCM from Climator Sweden AB. It is also discussed how the model can be used to compute apparent (effective) PCM properties in the phase transition temperature range, i.e. specific heat, density and thermal conductivity. Finally, simulation studies illustrate how the consideration of hysteresis affects the absorption and release of heat in a latent thermal energy storage system.

2. The two-phase model and apparent PCM properties

Phase transitions are modelled based on the general assumption, that the overall structure of the PCM can be approximated by two phases, a solid and a liquid phase. For technical grade PCM the phase change does not occur at an exact temperature, but rather within a specific temperature range. This means that it is assumed that the two phases coexist during solid/liquid phase transition and allows to approximate the overall structure of the PCM by one characteristic parameter $\xi \in [0,1]$,

$$\xi := \frac{m^l}{m^l + m^s} \qquad \text{Eq. 1}$$

denoting the (liquid mass) phase fraction, and m^s and m^l are the masses of solid and liquid phase, respectively.

Within the phase transition temperature range the PCM thermophysical properties are modelled by a linear superposition of contributions from pure solid and pure liquid PCM properties. This superposition gives so called 'apparent' (or effective) PCM properties. These apparent properties are denoted here by the symbol '~'. The apparent density $\tilde{\rho}$ and thermal conductivity $\tilde{\lambda}$ property models read:

$$\tilde{\rho} := \xi \, \rho^l + (1 - \xi) \, \rho^s \qquad \text{Eq. 2}$$

$$\tilde{\lambda} := \xi \, \lambda^l + (1 - \xi) \, \lambda^s \qquad \text{Eq. 3}$$

and the phase fraction ξ is used to compute the weights of the contribution from pure liquid and solid. In the same way, the apparent specific heat capacity $\tilde{c}$ is given by a linear superposition of pure liquid and solid heat capacity as well as the latent heat (Δh) released or absorbed in the phase transition region (Gaur and Wunderlich 1981):

$$\tilde{c} := \underbrace{\xi \, c_p^l + (1 - \xi) c_p^s}_{\text{sensible heat}} + \underbrace{\frac{d\xi}{dT} \Delta h}_{\text{latent heat}} \qquad \text{Eq. 4}$$

Enthalpy-temperature relations $h(T)$ are obtained by integration:

$$h(T) - h(T_{\text{ref}}) = \int_{T_{\text{ref}}}^{T} \tilde{c}(\tau) \, d\tau \qquad \text{Eq. 5}$$

where it is assumed that T_{ref} is much smaller than the temperatures defining the phase transition temperature range.

3. PCM phase transition models

The phenomenological modelling approach is based on the determination of complete phase transitions (between solid, with phase fraction $\xi = 0$, and liquid, with $\xi = 1$).

3.1 Complete phase transitions

Most simple models for complete phase transitions assume that the phase fraction is a direct function of temperature: $\xi := \xi(T)$.

Assumption: It is assumed that ξ monotonously increases with rising temperature T and that the transition from $\xi = 0$ to $\xi = 1$ is smooth.   Eq. 6

Following the assumption above, cumulative distribution functions seem convenient to be used to model phase transitions:

$$\xi(T) := \int_{-\infty}^{T} \phi(\tau)\, d\tau \quad \text{with} \quad \int_{-\infty}^{\infty} \phi(\tau)\, d\tau = 1 \qquad \text{Eq. 7}$$

where $\phi(T)$ is a (continuous) probability distribution function (PDF), and $\xi(T)$ is the corresponding cumulative distribution function. There is a variety of distribution functions with different shapes (see e.g. Croarkin and Tobias 2006) which can be parametrized by a relatively small number of location and shape parameters. This is especially useful when fitting phase transition models to experimental data by numerical solution of a nonlinear regression problem. In this contribution, the Gumbel Minimum distribution ϕ^G and its cumulative distribution function are used:

$$\phi^G(T;\mu,\beta) = \frac{1}{\beta} \exp\left(\frac{T-\mu}{\beta}\right) \exp\left(- exp\left(\frac{T-\mu}{\beta}\right)\right)$$

$$\int_{-\infty}^{T} \phi^G(\tau;\mu,\beta)\, d\tau = 1 - \exp\left(- exp\left(\frac{T-\mu}{\beta}\right)\right) \qquad \text{Eq. 8}$$

where T is the temperature in K, and μ, β are the respective location and shape parameters. The Gumbel Minimum distribution was found useful for representing the asymmetric peak of the studied ClimSel PCM.

3.2 Incomplete phase transitions with hysteresis

The phase transition model in Eq. 7 is able to predict phase transitions where the PCM undergoes either complete solid-to-liquid phase change described by $\xi^{s \to l}(T)$, or complete liquid-to-solid phase change described by $\xi^{l \to s}$, see Eq. 9.

$$\xi(T) := \xi^{s \to l}(T) \qquad \text{for complete melting}$$

$$\xi(T) := \xi^{l \to s}(T) \qquad \text{for complete solidification}$$

Eq. 9

The model does not account for incomplete phase transitions. This means that switches between heating and cooling operation while the material is still within the phase transition range (phase transition is not completed), do not result in a change of the phase transition curve.

The studied 'curve scale' hysteresis model, taken from Ivshin and Pence 1994, is completely defined by $\xi^{s \to l}(T)$ and $\xi^{l \to s}(T)$. The decision on the model to be used depends on the sign of the temperature rate. This means that there exists one model 'for heating' with $\text{sgn}(dT/dt) > 0$, and one model 'for cooling' with $\text{sgn}(dT/dt) < 0$. As the name suggests, after changes in the direction of the temperature rate during incomplete phase transitions, both models scale the transition functions. The scaling depends on the pair of values (T_0, ξ_0) at the last switching point, with $\xi_0 = \xi(T_0)$. The hysteresis model reads:

$$\xi := \xi\left(T, \text{sgn}\left(\frac{dT}{dt}\right)\right) = \begin{cases} \xi(T) := 1 - \dfrac{1 - \xi(T_0)}{1 - \xi^{s \to l}(T_0)} \cdot \left(1 - \xi^{s \to l}(T)\right) & \text{for heating} \\[4mm] \xi(T) := \dfrac{\xi(T_0)}{\xi^{l \to s}(T_0)} \cdot \xi^{l \to s}(T) & \text{for cooling} \end{cases} \qquad \text{Eq. 10}$$

4. Identification of phenomenological phase transition models with hysteresis

In the following, a workflow for the derivation of phase transition models from PCM heat capacity data is proposed and applied to model two commercial PCM.

4.1 Workflow for the model identification

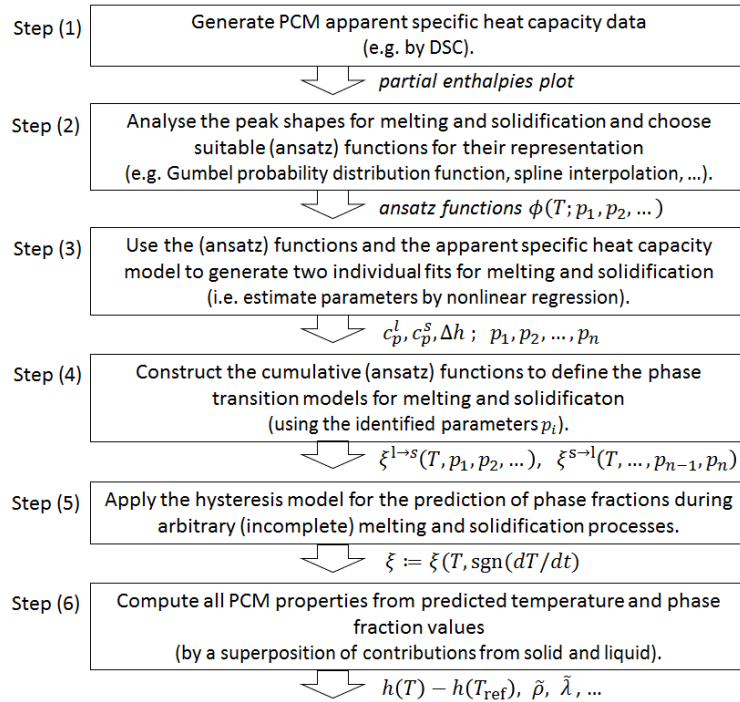The proposed workflow is shown in Figure 1.

Figure 1. Proposed workflow for the identification of phenomenological phase transition models with hysteresis and the computation of PCM properties during partial melting and solidification.

It is assumed that PCM specific heat capacity data is available (as partial enthalpies) for the phase transition temperature range, see **step (1)** in Figure 1. This data is usually provided by the manufacturer, i.e. in the PCM datasheets. In **step (2)**, the plots showing partial enthalpies over temperature are analysed and two suitable (ansatz) functions are chosen, which can reproduce the observed characteristics of the enthalpy peak for heating (melting) and cooling (solidification) in the phase transition temperature range. The focus for the selection should be on the reproduction of (possibly) asymmetric peak shapes, i.e. left-skewed, right-skewed. Moreover, bimodal or even multiple modes might be considered by superposition of two, or multiple transition functions. In **step (3)**, the apparent specific heat capacity model is used with the selected (ansatz) functions. The model is fitted (individually) to the partial enthalpy data for heating and cooling. This fitting might be performed by numerical solution of a non-linear regression problem. The results are the sensible and latent heat, and additional parameters of the (ansatz) functions. In **step (4)**, the cumulative (ansatz) functions are used to define the phase transition models for complete melting and solidification. In **step (5)**, these phase transition models are combined with the hysteresis model in Eq. 10. The hysteresis model is then used to predict phase fraction evolutions for arbitrary, complete and incomplete melting and solidification processes. Finally, in **step (6)**, the PCM properties are computed from temperature and corresponding phase fraction values.

4.2   *Application of the workflow for PCM ClimSel C58 and C48*

The workflow in Figure 1 is exemplarily applied for modelling two commercial PCM, namely ClimSel C58 and C48 from Climator Sweden AB.

Step (1): Partial enthalpy data as given in the PCM data sheets are depicted by triangles in Figure 2 (left) and Figure 3 (left).

Step (2): Gumbel Minimum distribution ϕ^G in Eq. 8 is chosen as an (ansatz) function. The fitting parameters are μ and β.

Step (3): Using Gumbel Minimum distribution, the apparent specific heat capacity model is fitted to the partial enthalpy data. For ClimSel C58, the following regression parameters are found: for heating $\mu = 58.0°C$, $\beta = 0.64$; for cooling $\mu = 54.9°C$, $\beta = 0.55$. The estimated heat capacity and latent heat values are: $c_p^s = 4.7$ kJ/(kg·K), $c_p^l = 2.2$ kJ/(kg·K) and $\Delta h = 200.7$ kJ/kg. For ClimSel C48, the following regression parameters are found: for heating $\mu = 50.6°C$, $\beta = 2.26$; for cooling $\mu = 47.3°C$, $\beta = 0.84$. The estimated heat capacity and latent heat values are: $c_p^s = 6.8$ kJ/(kg·K), $c_p^l = 3.3$ kJ/(kg·K) and $\Delta h = 97.5$ kJ/kg. The results, i.e. the fitting functions are shown in Figure 2 (left) and Figure 3 (left) as continuous lines. Moreover, Figure 4 shows details for the fitted apparent specific heat capacity model for ClimSel C48, namely the contributions from sensible and latent heat.
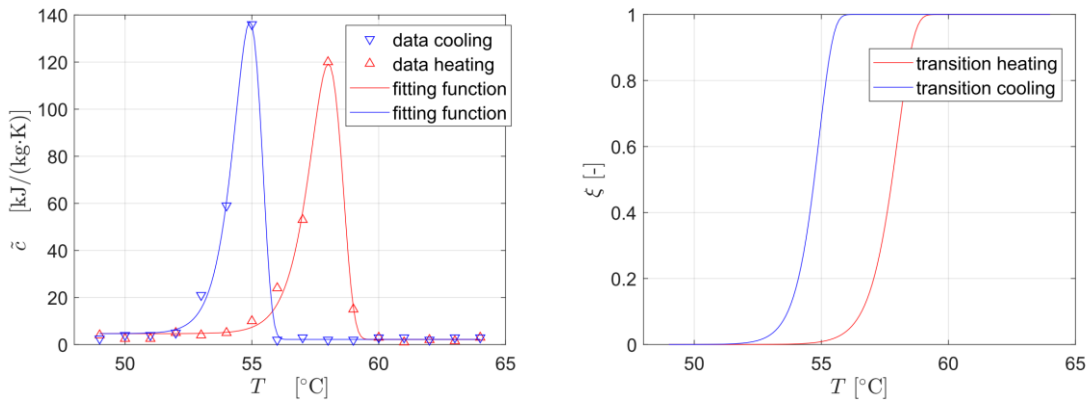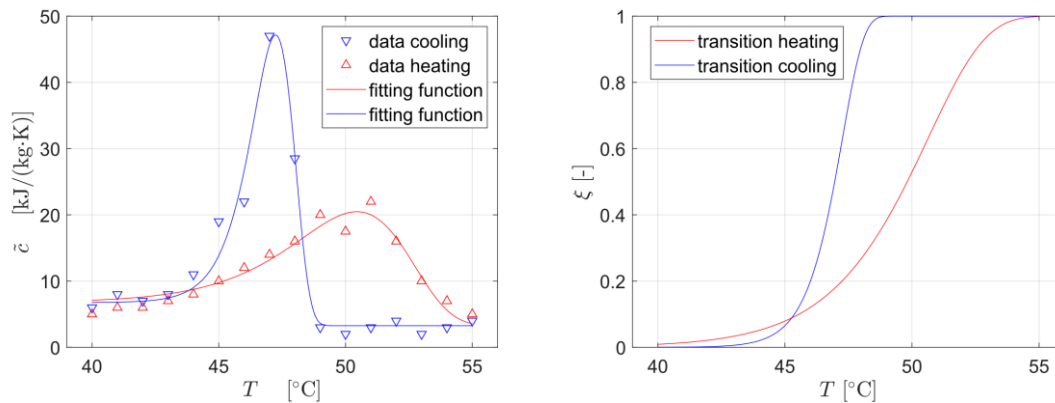

Figure 2. Fitting partial enthalpies for ClimSel C58 (data taken from Climator Sweden AB). Peak data for heating and cooling is fitted individually. Left: Fitting functions for apparent specific heat capacity. Right: The corresponding phase transition functions for heating $\xi^{s \to l}$ and cooling $\xi^{l \to s}$ using Gumbel Minimum distributions.

Figure 3. Fitting partial enthalpies for ClimSel C48 (data taken from Climator Sweden AB). Peak data for heating and cooling is fitted individually. Left: Fitting functions for apparent specific heat capacity. Right: The corresponding phase transition functions for heating $\xi^{s \to l}$ and cooling $\xi^{l \to s}$ using Gumbel Minimum distributions.
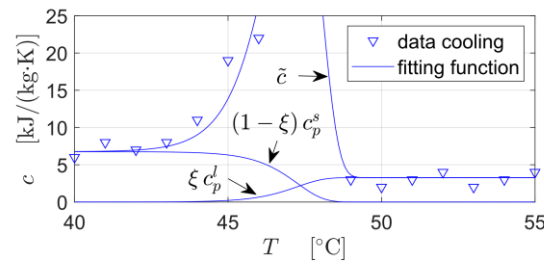
Figure 4. Details on the fitting of heat capacity data for ClimSel C48 as shown in Figure 3. Results are shown for cooling data only, for the apparent specific heat capacity $\tilde{c}$, the weighted liquid $\xi\, c_p^l$, and the weighted solid $(1-\xi)c_p^s$ heat capacity, see Eq. 4.

Step (4): Using the identified Gumbel Minimum distribution parameters the cumulative distribution is used to compute the evolution of the phase fractions during complete melting (heating) and solidification (cooling). The results are shown in Figure 2 (right) and Figure 3 (right).

Step (5): The hysteresis model is now completely defined by $\xi^{s\rightarrow l}$ and $\xi^{l\rightarrow s}$. Figure 5 (left) and Figure 6 (left) show the predicted phase fractions for PCM temperature variations (consecutive heating and cooling) starting from a solid PCM state and finally reaching the liquid state. Switching points between heating and cooling imply a switch between the two models in Eq. 10 and are marked by a circle and numbered as 1, 2, 3, and 4. Moreover, on the right side of Figure 5 and Figure 6 the same results in the (T, ξ)-plane are shown.
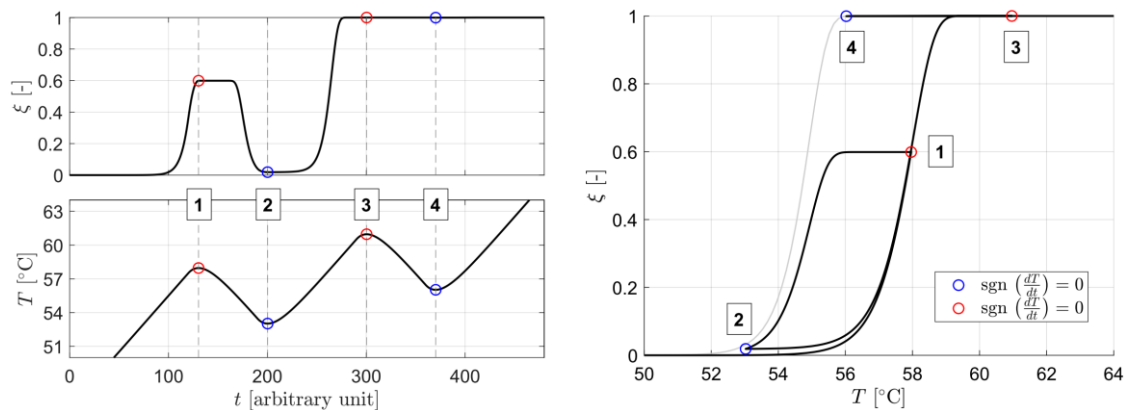

Figure 5. Predicted temperature induced phase transitions for 'curve scale' hysteresis model using identified phase transition functions for ClimSel C58. Left below: Applied temperature variations. Switching points between heating and cooling are marked by a circle and numbered as 1, 2, 3, and 4. Left above: Predicted phase fraction evolution. Right: Predictions in the (T, ξ)-plane. Note that time is given in arbitrary units, as the results are independent of the rate of temperature variations.
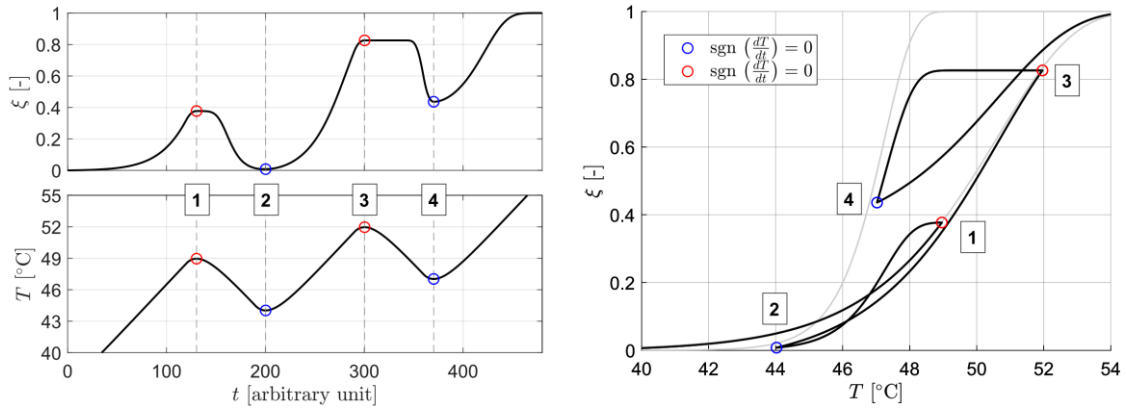
Figure 6. Predicted temperature induced phase transitions for 'curve scale' hysteresis model using identified phase transition functions for ClimSel C48. Left below: Applied temperature variations. Switching points between heating and cooling are marked by a circle and numbered as 1, 2, 3, and 4. Left above: Predicted phase fraction evolution. Right: Predictions in the (T, ξ)-plane. Note that time is given in arbitrary units, as the results are independent of the rate of temperature variations.

Step (6): Figure 7 depicts the evolution of the predicted apparent thermal conductivity and enthalpy for the consecutive heating and cooling scenario shown in Figure 6 and Figure 5. Figure 7 (left) shows the results for ClimSel C58, Figure 7 (right) for ClimSel C48.

Comparing the predictions for the hysteresis model $\xi(T, \mathrm{sgn}(dT/dt))$, and for the simple phase transition models for heating $\xi^{s \to l}(T)$, and cooling $\xi^{l \to s}(T)$, large differences can be seen in the computed values after switching between heating and cooling while still being in the phase transition temperature range, i.e. while the phase transitions are incomplete.
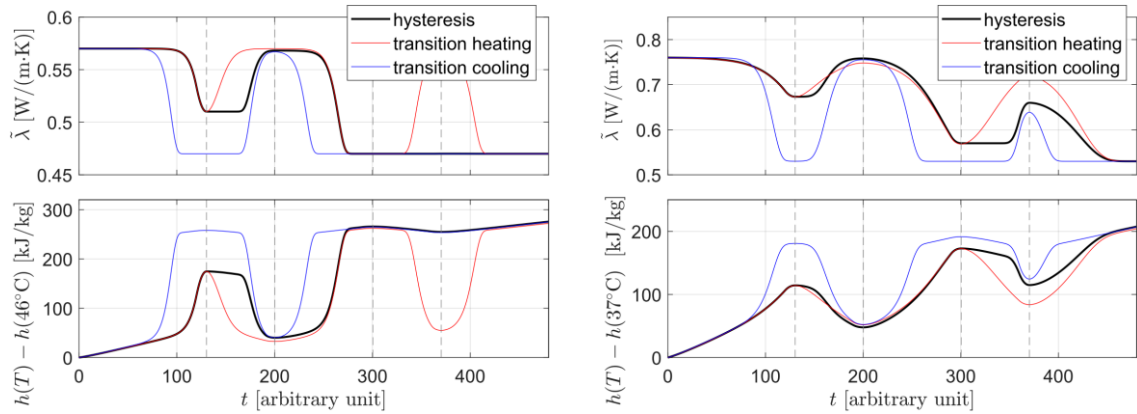

Figure 7. Predicted evolutions for the apparent thermal conductivity and enthalpy for the consecutive heating and cooling scenario shown in Figure 5 and Figure 6. Results are shown for the hysteresis model $\xi(T, \mathrm{sgn}(dT/dt))$ in Eq. 10, and for the simple phase transition models for heating $\xi^{s \to l}(T)$ and cooling $\xi^{l \to s}(T)$.

5. Conclusions

This contribution proposes a generic workflow for the identification of solid/liquid PCM phase transition hysteresis models, where the hysteresis in phase fraction originates from positive (heating) and negative (cooling) temperature rates and the temperature history. The phenomenological modelling approach uses PCM heat capacity data, i.e. partial enthalpies, as usually provided in the data sheets of PCM manufacturers.

In contrast to other works which characterize the phase transition behaviour by enthalpy-temperature curves $h(T)$, this contribution uses (liquid mass) phase fraction-temperature curves

$\xi(T)$. In doing so, within the phase transition temperature range, all thermo-physical PCM properties are modelled by a superposition of pure solid and pure liquid PCM properties, where these pure properties are often also available from manufacturer data sheets. The predicted PCM properties are then so called apparent (effective) properties, e.g. apparent specific heat capacity, density or thermal conductivity.

The workflow for the identification of phenomenological models seems especially attractive, as:

- it relies on data which is typically available for commercial PCM,
- it combines different information for complete melting (heating) and solidification (cooling) experiments in one model,
- it generates a model for the analysis of hysteresis effects during incomplete melting and solidification and arbitrary switches between heating and cooling.

For these advantages, the presented hysteresis model seems especially useful for the characterization of latent thermal energy storages with PCM showing significant hysteresis and operating under partial load conditions. The effort for the generation of this phenomenological model is also small compared to the effort for the development of a mechanistic (kinetic, rate-dependent) model including complex nucleation and crystal growth mechanisms.

However, there is also a critical limitation of the hysteresis model used in this contribution:

- it is a 'static' model, which means that it is rate-independent. Thus, increased heating rates directly lead to faster melting, but they also result in the same magnitude of the hysteresis, contrary to experimental findings, see e.g. Diaconu and Cruceru 2010.

Because of this (and the assumption in Eq. 6), it is not possible to analyse supercooling, i.e. spontaneous release of heat while cooling, using the presented hysteresis model. However, the analysis of predicted and experimental PCM temperatures in a latent heat thermal energy storage operated under partial load conditions clearly indicate a superior performance of the presented hysteresis model when compared to conventional models based on heat capacity data for heating or cooling only (Barz and Sommer 2018).

Acknowledgements

References

Al-Saadi, S. N.; Zhai, Z. J. (2013): Modeling phase change materials embedded in building enclosure: A review. In *Renewable and Sustainable Energy Reviews* 21, pp. 659–673.

Barz, T.; Sommer, A. (2018): Modeling hysteresis in the phase transition of industrial-grade solid/liquid PCM for thermal energy storages. In *International Journal of Heat and Mass Transfer* 127, pp. 701–713.

Biswas, K.; Shukla, Y.; Desjarlais, A.; Rawal, R. (2018): Thermal characterization of full-scale PCM products and numerical simulations, including hysteresis, to evaluate energy impacts in an envelope application. In *Applied Thermal Engineering* 138, pp. 501–512.

Bony, J.; Citherlet, S. (2007): Numerical model and experimental validation of heat storage with phase change materials. In *Energy and Buildings* 39 (10), pp. 1065–1072.

Climator Sweden AB: ClimSel product data sheets. Available online at https://www.climator.com/en/pcm-climsel/product-data-sheets, checked on 02/2019.

Croarkin, Carroll; Tobias, Paul (2006): NIST/SEMATECH e-handbook of statistical methods. Available online at http://www.itl.nist.gov/div898/handbook/.

Diaconu, B.M.; Cruceru, M. (2010): Novel concept of composite phase change material wall system for year-round thermal energy savings. In *Energy and Buildings* 42 (10), pp. 1759–1772.

Diaconu, B.M.; Varga, S.; Oliveira, A.C. (2010): Experimental assessment of heat storage properties and heat transfer characteristics of a phase change material slurry for air conditioning applications. In *Applied Energy* 87 (2), pp. 620–628.

Gasia, J.; Gracia, A. de; Peiró, G.; Arena, S.; Cau, G.; Cabeza, L.F. (2018): Use of partial load operating conditions for latent thermal energy storage management. In *Applied Energy* 216, pp. 234–242.

Gaur, U.; Wunderlich, B. (1981): Heat capacity and other thermodynamic properties of linear macromolecules. II. Polyethylene. In *J. Phys. Chem. Ref. Data* 10 (1), p. 119.

Goia, F.; Chaudhary, G.; Fantucci, S. (2018): Modeling and experimental validation of an algorithm for simulation of hysteresis effects in phase change materials for building components. In *Energy and Buildings*.

Gowreesunker, B. L.; Tassou, S. A. (2013): Effectiveness of CFD simulation for the performance prediction of phase change building boards in the thermal environment control of indoor spaces. In *Building and Environment* 59, pp. 612–625.

Hu, Y.; Heiselberg, P.K. (2018): A new ventilated window with PCM heat exchanger—Performance analysis and design optimization. In *Energy and Buildings* 169, pp. 185–194.

Ivshin, Y.; Pence, T.J. (1994): A constitutive model for hysteretic phase transition behavior. In *International Journal of Engineering Science* 32 (4), pp. 681–704.

Kumarasamy, K.; An, J.; Yang, J.; Yang, E. (2017): Novel CFD-based numerical schemes for conduction dominant encapsulated phase change materials (EPCM) with temperature hysteresis for thermal energy storage applications. In *Energy* 132, pp. 31–40.

Moreles, E.; Huelsz, G.; Barrios, G. (2018): Hysteresis effects on the thermal performance of building envelope PCM-walls. In *Building Simulation* 11 (3), pp. 519–531.

Rose, J.; Lahme, A.; Christensen, N. U.; Heiselberg, P.; Hansen, M.; Grau, K. (2009): Numerical method for calculating latent heat storage in constructions containing phase change material. In: Proceedings of building simulation 2009: 11th conference of the international building performance simulation association. Eleventh International IBPSA Conference. Glasgow, Scotland, GBR, July 27-30, pp. 400–407.

Uzan, A.Y.; Kozak, Y.; Korin, Y.; Harary, I.; Mehling, H.; Ziskind, G. (2017): A novel multi-dimensional model for solidification process with supercooling. In *International Journal of Heat and Mass Transfer* 106, pp. 91–102.